# Anatomy of a Real-Life Non-Linear Device: Hydraulic Engine Mount

Rajendra Singh <singh.3@osu.edu> and Song He <he.81@osu.edu>
Acoustics and Dynamics Laboratory, Department of Mechanical Engineering and Center for Automotive Research, The Ohio State University, Columbus, OH 43210 USA

**ABSTRACT**

Hydraulic engine mount is infested with continuous and discontinuous non-linearities and accordingly its parameters significantly vary with the amplitude and frequency of sinusoidal excitation. Typical non-linear characteristics include the non-linear chamber compliances, vacuum formation in the top chamber during the expansion process, non-linear fluid resistances and the switching mechanism of the decoupler. In this paper, we review the historical progress made in the identification and modeling of non-linear dynamic behavior of free and fixed decoupler mounts. Basic concepts, mathematical models and bench tests are summarized. New discontinuous models of top and bottom chamber compliances (depending on the operating point and/or dynamic loading) are briefly proposed. In particular, explicit and implicit non-linearities under realistic excitation conditions are addressed, especially when the mean load itself also varies with time, and when several dynamic (sinusoidal and/or transient) excitations are simultaneously present. Finally, transient response predictions are compared with measurements and the role of multi-staged and time-varying chamber compliances is explained.

## 1. Introduction

In this article, we will examine the anatomy of a real-life device, hydraulic engine mount. It is designed to be highly non-linear as its parameters, such as stiffness and damping parameters, significantly vary with the amplitude ($X$) and frequency ($f$) of sinusoidal excitation [1]. For a free decoupler type mount as shown in Fig. 1, one should expect the following elements to exhibit non-linear behavior [1-16]: First, multi-staged top chamber (#1) compliance $C_1(p_1)$ where $p_1(t)$ is the dynamic chamber pressures and $t$ is time [1-3]; Second, the switching mechanism of the decoupler ($d$) [2-3,14-16]; Third, non-linear resistances $R_i(q_i)$ and $R_d(q_d)$, where $q_i(t)$ and $q_d(t)$ are the volumetric flow rates through the inertia track ($i$) and decoupler, respectively [1,10,14-16]; Fourth, lower chamber (#2) compliance $C_2(F_m)$ which varies with preload $F_m$ [10]. Additional non-linearities could include the elastomer non-linearity and squeeze-film effect [4,15], etc. Since Kim and Singh [2-3] initiated the non-linear analysis of hydraulic mounts in early 1990s, much research has been conducted over the past 15 years. Some of the prior work has been summarized by Yu et al. [8], who conducted a literature survey of vehicle engine mounting systems and pointed out the superiority of hydraulic mounts over conventional elastomeric mounts due to frequency- and amplitude-dependency. In this article, we will first review and categorize the historical progress that has been made in understanding and quantifying the mount non-linearities using laboratory experiments and mathematical models. Both explicit and implicit displacement non-linearities under realistic excitation conditions will be addressed. New discontinuous $C_1(p_1)$ and $C_2(F_m)$ models will then be proposed to explain those non-linearities which are excited under transient or arbitrary loading conditions (say with time-varying mean load and/or multiple frequency components). Finally, typical comparisons between nonlinear models and experiments will be presented.

## 2. Non-linear studies of hydraulic mount

### *2.1. Review of non-linear experiments and models*

A historical review is summarized in Table 1 with focus on the non-linear modeling and associated bench tests. Kim and Singh [2-3] first measured the non-linear $C_1$, $C_2$ and $R_i$ of a fixed decoupler mount via bench experiments. They also successfully formulated a non-linear model that included a preliminary formulation for the decoupler switching mechanism under harmonic excitations [3]. Colgate et al. [4] tested several mounts under dual sinusoidal excitations and proposed two separate linear models for large and small amplitudes. Royston and Singh [5,6] employed Kim and Singh's model [3] as a localized non-linearity and examined its effect on the vibratory power transmission. Jeong and Singh [7] suggested a non-linear time domain model based on a quasi-linear model with frequency- and amplitude-dependent parameters. Empirical coefficients were obtained by observing the changes in resonant frequencies and viscous damping ratios given measured mount stiffness $K(f, X)$

data. Further, Geisberger et al. [8, 10] tested fluid chamber compliances, inertia track and decoupler parameters. They proposed a non-linear model that utilizes a smoothening function to describe the decoupler switching phenomenon. Jazar and Golnaraghi [11] proposed a simple non-linear mathematical model to characterize the decoupler resistance in terms of the Duffing's equation (continuous non-linearity). This leads to semi-analytical solutions using the multiple scale perturbation method and thus the jump phenomenon at resonance could be studied. Foumani et al. [13] conducted a sensitivity analysis and concluded that $C_1$ and $I_i$ are the most influential parameters in the dynamic stiffness model over the lower frequency range, while $C_1$ and decoupler inertia $m_d$ are most critical at higher frequencies. Tiwari et al. [14] refined the bench experiments that were initially proposed by Kim and Singh [3] and further quantified $C_1$ and $C_2$ parameters under several $F_m$ values. Also, they investigated the vacuum formation that was first observed by Kim and Singh [2-3]. Adiguna et al. [15] examined the mount behavior to idealized transient excitations and successfully predicted the transient responses based on non-linear formulations with experimentally characterized parameters or functions. Recently, we [17] proposed an efficient procedure to estimate the frequency- and amplitude-sensitive parameters of a quasi-linear model based on measured steady state $K(f, X)$ data. Likewise, Lee and Kim [18] have proposed an equivalent viscous damping expression for inertia track based on a non-linear model. The quasi-linear models [17] are capable of partially predicting simple transient response [19] but they may not work when the operational conditions (and thus mount parameters) vary significantly with time. Choi et al. [12] examined the electronically controllable electro-rheological (ER) engine mount. Foumani et al. [16] proposed a tunable hydraulic mount design by adjusting the inertia track length and/or effective decoupler area. Further discussion of adaptive and active mounts is beyond the scope of this article.

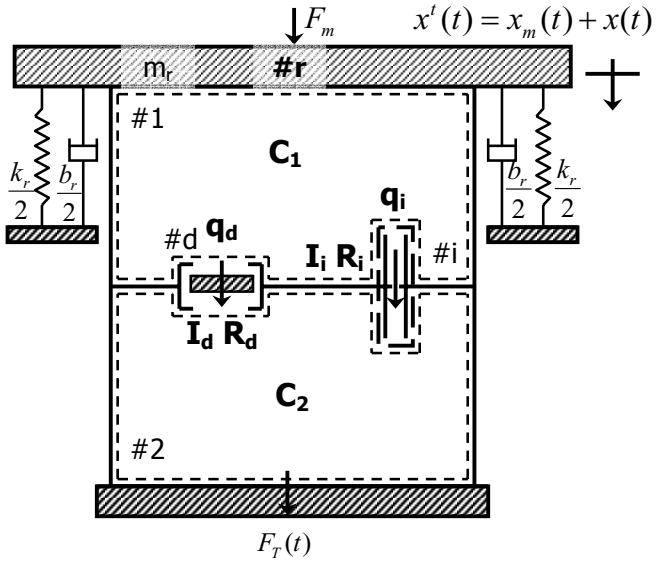


Fig. 1 Lumped fluid model of a free decoupler mount with inertia track (subscript *i*) and decoupler (subscript *d*). Here, $F_m$ is the preload; $F_T(t)$ is the transmitted force; $x$ is the displacement excitation; $m_r$ is the mass of rubber element; $k_r$ and $b_r$ are the rubber element stiffness and damping coefficient; and symbols $C$, $I$, $q$, $R$ correspond to chamber compliance, fluid inertia, volumetric flow rate and fluid resistance, respectively.

*2.2. Fluid system formulation*

In this paper, we will summarize only those equations that are necessary for further development of the non-linear lumped fluid model of Fig. 1. Considering only the time-varying components, the "virtual" driving point force $F(t)$ could be defined as follows where $x(t)$ is the piston displacement and $A_r$ is the effective piston area [17].

$$F(t) = m_r\ddot{x}(t) + b_r\dot{x}(t) + k_r x(t) + A_r p_1(t) \tag{1}$$

Continuity equations for the top and bottom chambers of Fig. 1 yield:

$$A_r\dot{x}(t) - q_i(t) - q_d(t) = C_1(p_1)\dot{p}_1(t), \qquad q_i(t) + q_d(t) = C_2(F_m)\dot{p}_2(t) \tag{2, 3}$$

Momentum equations for the decoupler and inertia track yield the following:

$$p_1(t) - p_2(t) = I_d\dot{q}_d(t) + R_d(q_d)q_d(t), \qquad p_1(t) - p_2(t) = I_i\dot{q}_i(t) + R_i(q_i)q_i(t) \tag{4, 5}$$

Table 1 Identification and quantification of hydraulic engine mount non-linearities

| Non-Linear component or system | Investigators [reference number] | Measurements conducted to identify and quantify non-linearities | Modeling of non-linear component, process or system |
|---|---|---|---|
| Decoupler kinematic or flow characteristics | Kim and Singh [2-3] | $p_1(t)$ | Switching model controlled by decoupler volume |
| | Royston and Singh [5-6] | -- | Non-linear decoupler spring with softening effects |
| | Geisberger et al. [8,10] | $R_d$ leakage resistance $R_d'$ etc. | Flow model using smoothening function |
| | Jazar and Golnaraghi [11] | $K(f,X)$ elastomer test | $R_d$ model using Duffing's equation |
| | Tiwari et al. [14] | $p_1(t)$, $F_T(t)$; transient tests | Switching model controlled by relative decoupler position; squeeze film model |
| | Adiguna et al. [15] | | |
| | He and Singh [20] | Harmonic and transient tests | Implicit decoupler excitation model |
| Top chamber compliance $C_1$ | Kim and Singh [2-3] | Multiple regression of $C_1(p_1)$, $p_1(t)$ polynomials | Two-stage model including vacuum formation |
| | Tiwari et al. [14] | | |
| | Geisberger et al. [8,10] | Linear curve fit of $C_1(f,X)$ | $C_1(f,X)$ model |
| | Foumani et al. [13] | -- | Sensitivity analysis of $C_1$ |
| | He and Singh [20] | Step up and down tests | Three-stage model including vacuum and hardening effects |
| Inertia track resistance | Kim and Singh [2-3] | Multiple regression and least-square curve-fit of $R_i(q_i)$ | Fluid model including leakage flow |
| | Tiwari et al. [14] | | $R_i(q_i)$ model |
| | Adiguna et al. [15] | | |
| | Royston and Singh [5,6] | -- | Semi-analytical model using Galerkin technique |
| | Geisberger et al. [8,10] | Least squares fit of $p_2 - p_1$ | Laminar and turbulent flow models |
| | Foumani et al. [13] | -- | Sensitivity analysis of $I_i$ |
| | Lee and Kim [18] | $K(f,X)$ elastomer test | Approximation of $R_i$ |
| Bottom chamber compliance $C_2$ | Kim and Singh [2-3] | Multiple regression of $C_2(p_2)$ polynomial | $C_2(p_2)$ model |
| | Tiwari et al. [14] | | |
| | Adiguna et al. [15] | | |
| | Geisberger et al. [8,10] | Curve-fit of $C_2(F_m)$ | $C_2(F_m)$ model |
| | He and Singh [20] | Transient tests with realistic input | $C_2(F_m)$ model with hardening effect |
| System level formulation (mounting or vehicle system) | Kim and Singh [1,3] | $K(f,X)$ elastomer test | Quarter-car model |
| | Colgate et al. [4] | | Piecewise linear model; squeeze-film model |
| | Jeong and Singh [7] | | Synthesis of local non-linearities in frequency domain; half-car model |
| | He and Singh [17,19] | | Quasi-linear model; analytical prediction of step responses |
| Adaptive and active mounts | Kim and Singh [3] | -- | Adaptive and active control models |
| | Choi and Song [12] | $K(f,X)$ elastomer test | ER fluid model; vehicle model with ER mount |
| | Foumani et al. [16] | -- | Tuning of inertia track length and decoupler area |

* Additional non-linear elements may include stiffness $k_r$ and viscous damping $b_r$ of the rubber element.

Note that Eq. (4) dictates the "decoupled" state when the decoupler gap is open, and Eq. (5) is dominant over the "coupled" state with the decoupler gap closes. The dynamic force transmitted to the rigid base is often viewed as a measure of mount performance in non-resonant tests [1]. Its dynamic component $F_T(t)$ is related to $F(t)$ as follows:

$$F_T(t) = k_r x(t) + b_r \dot{x}(t) + A_r p_1(t) = F(t) - m_r \ddot{x}(t) \tag{6}$$

## 3. Displacement excitations and associated non-linearities

### *3.1. Displacement excited non-linearities*

We classify explicit and implicit displacement excitation sources as: (i) an explicit composite excitation $x^t(t) = x_m(t) + x(t)$ externally applied and (ii) an implicit excitation due to the decoupler displacement $x_d(t)$. The mean component $x_m(t)$ is defined as the time-varying part $\Delta x(t)$ with same order of magnitude as the time-average of $x^t(t)$, and $x(t)$ corresponds to the fluctuation component. By examining typical excitations in Fig. 2, we will analyze the non-linearities that are excited by these. First, the sinusoidal excitation of Fig. 2(a) is commonly applied in dynamic stiffness measurement [1-16], where the constant $x_m$ under a specific preload $F_m$ is usually neglected in the analysis, leaving only the sinusoidal component $x(t) = X \cdot \sin(2\pi ft + \phi)$. In steady state elastomer tests, the dynamic stiffness is evaluated only at the frequency of excitation $f$ and super-harmonics are ignored [1-3]. Second, simple transient tests have been conducted under a constant $F_m$ (or time-invariant $x_m$), such as the triangular pulse excitation of Fig. 2(b) [10]. Transient responses to the special case of $x^t(t) = x_m(t) + x(t)$ have been partially predicted by the quasi-linear model [14]. This implies that for an idealized transient excitation when applied at a certain loading condition specified by $x_m$ (or $F_m$), the mount could behave as a linearized system and its effective parameters could be estimated by using the quasi-linear model [17]. Fourier series expansion may be employed for analyzing a periodic $x(t)$. Third, transient excitations with a rapid change in the mean loading condition such as the step-up excitation in Fig. 2(c) [14,17]. Significant asymmetries were observed in the measured peak values of $F_T(t)$ and $p_1(t)$ for the step-up and step-down responses, suggesting that a different non-linear stage has been introduced. Denoting $x_{m,1}$ and $x_{m,2}$ as the operating conditions before and after the switching event, the step-up (-down) excitation is formulated as follows, where $\Delta t$ represents the short time span during which the step function rises or drops (ideally $\Delta t \rightarrow 0$) due to the limitation of test facility:

$$x^t(t) = \begin{cases} x_{m,1} & 0 \le t < t_1 \\ x_{step}(\Delta t) & t_1 \le t < t_1 + \Delta t \\ x_{m,2} & t_1 + \Delta t < t \end{cases} \tag{7}$$

Fourth, the most complicated, yet realistic, excitations are considered, which may include the following terms: time-varying (say piece-wise linear) $x_m(t)$ and (ii) dynamic $x(t)$ with multiple and non-commensurate sinusoids at frequencies $f_i$ : $x^t(t) = x_{m,j-1} + \Gamma_i \left(t - t_{j-1}\right) + \sum_{i=1}^{n} X_i \sin(2\pi f_i t + \phi_i)$ . A constant slope $\Gamma_i = \left(x_{m,j} - x_{m,j-1}\right) / \left(t_j - t_{j-1}\right)$ is assumed within the $j^{th}$ segment, and a critical slope $\Gamma_c > \Gamma_i$ could be empirically chosen to distinguish $\Gamma_i$ from the rapid switching case of Eq. (7). The fluctuating part of $x(t)$ could be simplified by considering only the dominant sinusoidal excitation(s), say via the Fast Fourier Transform (FFT). The example case of Fig. 2(d) was measured at the mount location in a front wheel drive vehicle during a typical gear shift event. This transient record contains approximately 3 seconds of data. Several oscillatory displacements (from 5 to 15 Hz) are superimposed on $x_m(t)$ that increases from -4 to -10.5 mm, corresponding to a shift in $F_m$ from -1200 to -4000 N.

### *3.2. Implicit displacement excitation due to decoupler action*

The decoupler displacement $x_d(t)$ is dynamically coupled with instantaneous pressure difference $p_1(t) - p_2(t)$, excitation amplitude $X$, excitation frequency $f$ and decoupler gap length $l_g$. In time domain, the decoupler switching mechanism distorts the $p_1(t)$ and $F_T(t)$ waveforms (of a fixed decoupler mount) by introducing flattened regions whenever the decoupler gap opens. Consequently, $x_d(t)$ is categorized as an implicit displacement excitation. Fig. 3 shows the top camber pressure $P_1(f)$ and transmitted force $F_T(f)$ spectra for a take-apart mount with and without the decoupler excited by a sinusoidal excitation with $f$ = 12.5 Hz and $X$ = 0.5 mm (p-p), under $F_m$ = 1200 N (or $x_m$ = 3.7 mm). Compared with the $X(f)$ spectrum, the $X_d(f)$ spectrum of implicit excitation has discrete peaks not only at the external excitation frequency (12.5 Hz), but also at the 3rd harmonic and higher odd harmonics. Conversely, the peaks at the even harmonics are relatively smaller and remain almost unchanged. It is implied that $x_d(t)$ introduces an implicit excitation at the odd harmonics of external excitation frequency. Similar

phenomena could also be observed and analytically examined given the realistic excitation of Fig. 2(d). This will be reported in a new paper [20].

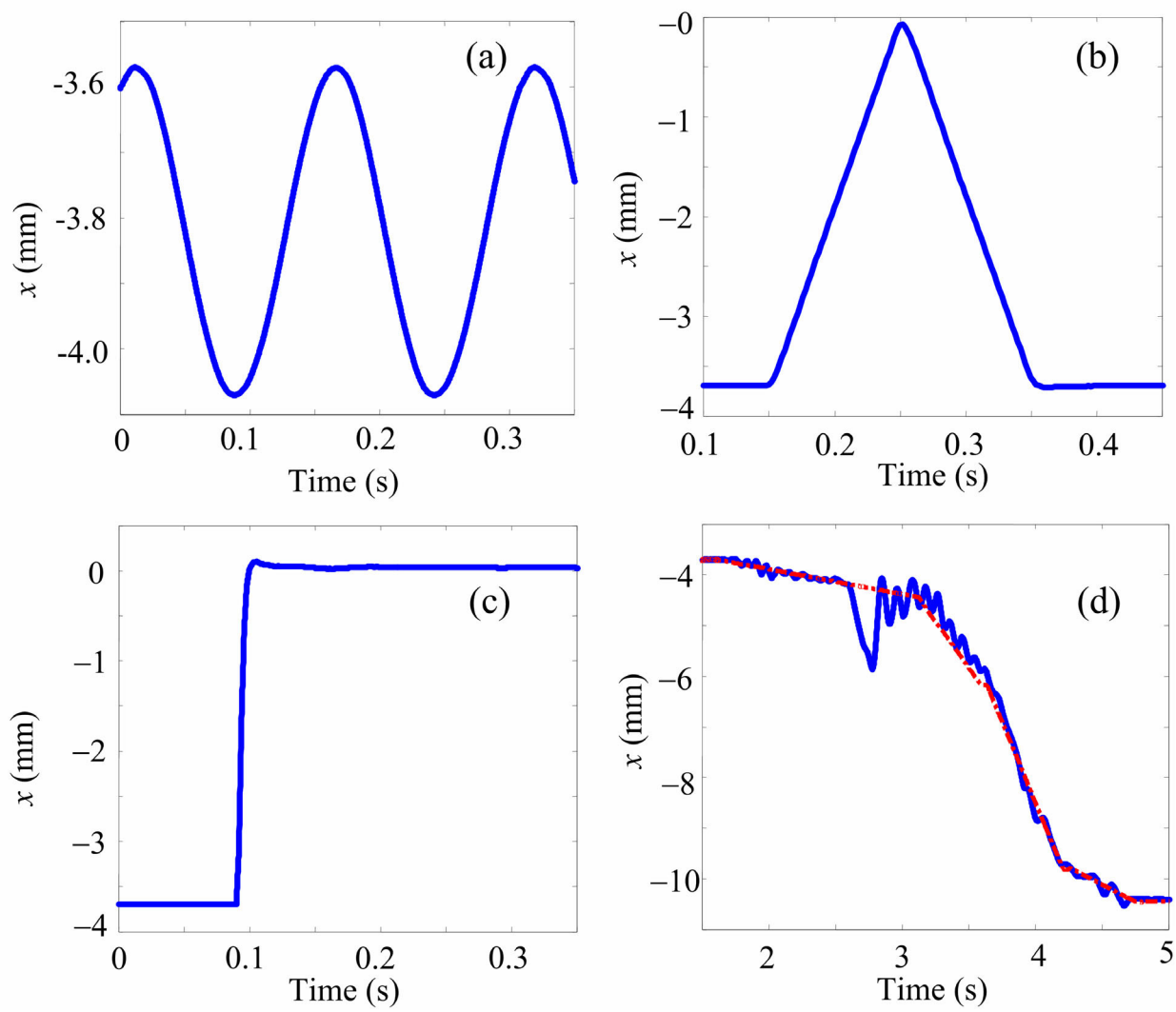


Fig. 2 Explicit displacement excitations: (a) sinusoidal excitation $x(t) = X \cdot \sin(2\pi ft + \phi)$; (b) simple triangular pulse excitation $x^t(t) = x_m(t) + x(t)$; (c) step-up excitation with a non-ideal rise; and (d) a realistic excitation from the measurements in a vehicle. Key for (d): ——, realistic $x^t(t)$; – · –, simplified (piecewise linear) mean displacement $x_m(t)$. Each excitation has been experimentally implemented but in some cases abrupt transitions are not seen due to the physical limitations of the test machine [14,15].

**4. Discontinuous $C_1(p_1)$ non-linearity**

By utilizing the quasi-linear model [17], two distinct effective $C_{1e}$ values could be estimated by best fitting the overshoot or decaying portions for several step-up and step down responses [14,15]. This allows us to estimate $C_1$ non-linearities and an interesting result emerges: $C_{1e}$ estimated from the overshoot of step-up response (from -3.7 to 0 mm) is consistent with statically measured $C_1$ under no preload; meanwhile, $C_{1e}$ estimated from the overshoot of step-down response (from 0 to -3.7 mm) coincides with measured $C_1$ under -1200 N preload (or $x_m$ = -3.7 mm). This suggests that the overshoots in step responses are closely related to the effective operating conditions after the step jump has occurred. Also, the nominal $C_{10}$ value, which is a linearized value based on several operational conditions, lies between the effective $C_{1e}$ values estimated from overshoots in step-up and step-down responses. This implies a dynamic softening effect associated with the unloading process, and a dynamic stiffening effect during the loading process. Kim and Singh [2] and Adiguna et al. [15] observed that the vacuum phenomenon is due to the release of dissolved gas during the expansion process. This gives rise to the dynamic softening effect, as mentioned earlier.

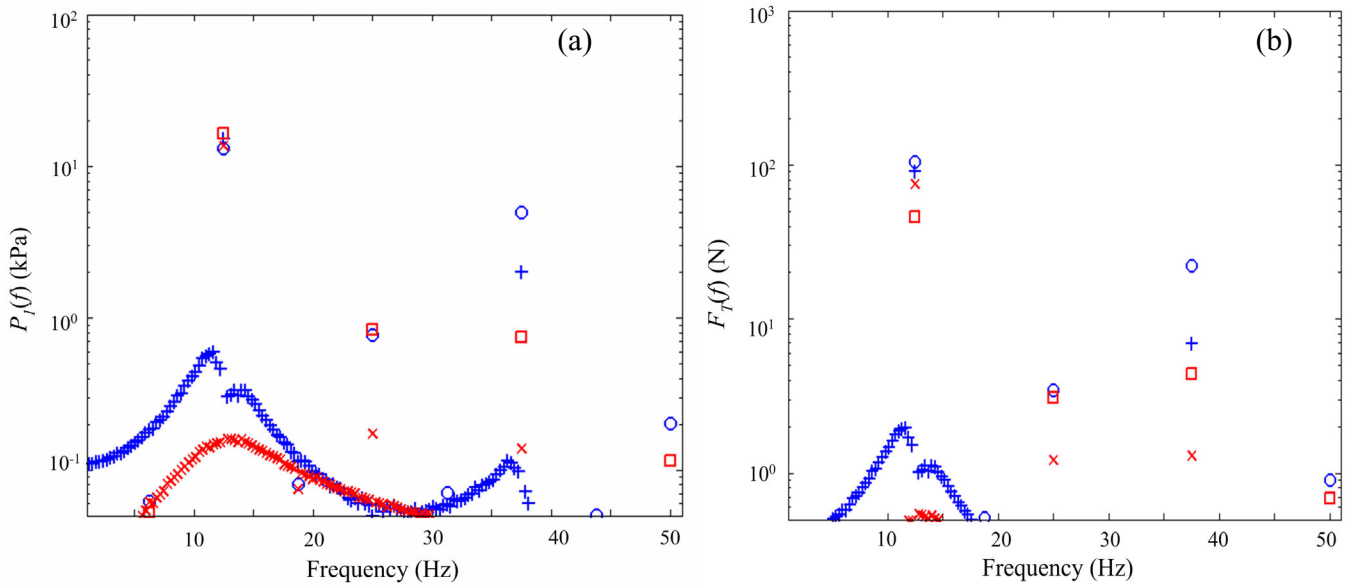


Fig. 3 Fourier amplitudes of $P_1(f)$ and $F_T(f)$ given a sinusoidal excitation with $f$ = 12.5 Hz and $X$ = 0.5 mm (p-p), under $F_m$ = 1200 N: (a) $P_1(f)$; (b) $F_T(f)$. Key: ○, measurement of free decoupler mount; +, measurement of fixed decoupler mount; □, simulation of free decoupler mount; ×, simulation of fixed decoupler mount.

By using $p_1(t)$ as an indicator of the operating condition, a multi-staged $C_1(p_1)$ model is proposed as follows to capture the asymmetric, mulit-staged non-linearity under vacuum, linear and dynamic loading conditions.

$$C_1(p_1) = \begin{cases} C_{10} - a_V p_1^{n_V}(t) & p_1(t) < 0 \ \text{(Vacuum Region)} \\ C_{10} & 0 \le p_1(t) \le p_a \ \text{(Linear Region)} \\ C_{10} - a_S \left[ p_1(t) - p_a \right]^{n_S} & p_a < p_1(t) \ \text{(Stiffening Region)} \end{cases} \quad (8)$$

Here, $C_{10}$ dictates the decaying response and $p_a$ is the limiting (atmospheric) pressure beyond which significant stiffening effect will occur. Empirical coefficients $a_V$ and $a_S$ and exponents $n_V$ and $n_S$ could be estimated from measurements. For instances, $a_V$ = 7e-45, $a_S$ = 1.55e-33, $n_V$ = 7, $n_S$ = 4 are estimated for one mount [14, 15]. Fig. 4(d) illustrates the predicted time-varying compliance $C_1(p_1)$ for a fixed decoupler mount. Observe that the stiffening effect occurs only during the loading process under the step-down (loading) process.

**5. Discontinuous $C_2(F_m)$ non-linearity**

The bottom chamber consists of a thin rubber membrane of irregular shape and it is intentionally designed to yield a large $C_2$ to accommodate the fluid displaced from the top chamber. Typically, $C_2$ >> $C_1$ by two orders of magnitude [2-3,14-15]. Due to the complex shape of the rubber bellow, an analytical calculation of $C_2$ is difficult but it can be curve-fitted from laboratory measurements. Most researchers [4-7] assume a linearized (constant) value of $C_2$ around a certain operating point that is specified by $F_m$. Adiguna et al. [15] and Kim and Singh [2-4] have briefly discussed the effects of $F_m$ on the chamber compliances. First, $F_m$ dictates the operating point about which the non-linear compliances are estimated. Second, $F_m$ determines the mean fluid pressure under the static equilibrium. However, when $F_m$ varies with time in some real-life operational conditions such as excitation of Fig. 2(d), a piecewise non-linear $C_2(F_m)$ or $C_2(x_m)$ as given by Eq. (9) must be utilized to fully capture the stiffening effect under higher $F_m$ (or $x_m$). This gives rise to a significant increase in the mean chamber pressure as observed in measurements. Detailed results including comparison with experiments will be reported in an upcoming paper [20].

$$C_2\left(F_m(t)\right) = C_{2,j-1} + \frac{C_{2,j} - C_{2,j-1}}{t_j - t_{j-1}}\left(t - t_{j-1}\right) \quad (9)$$

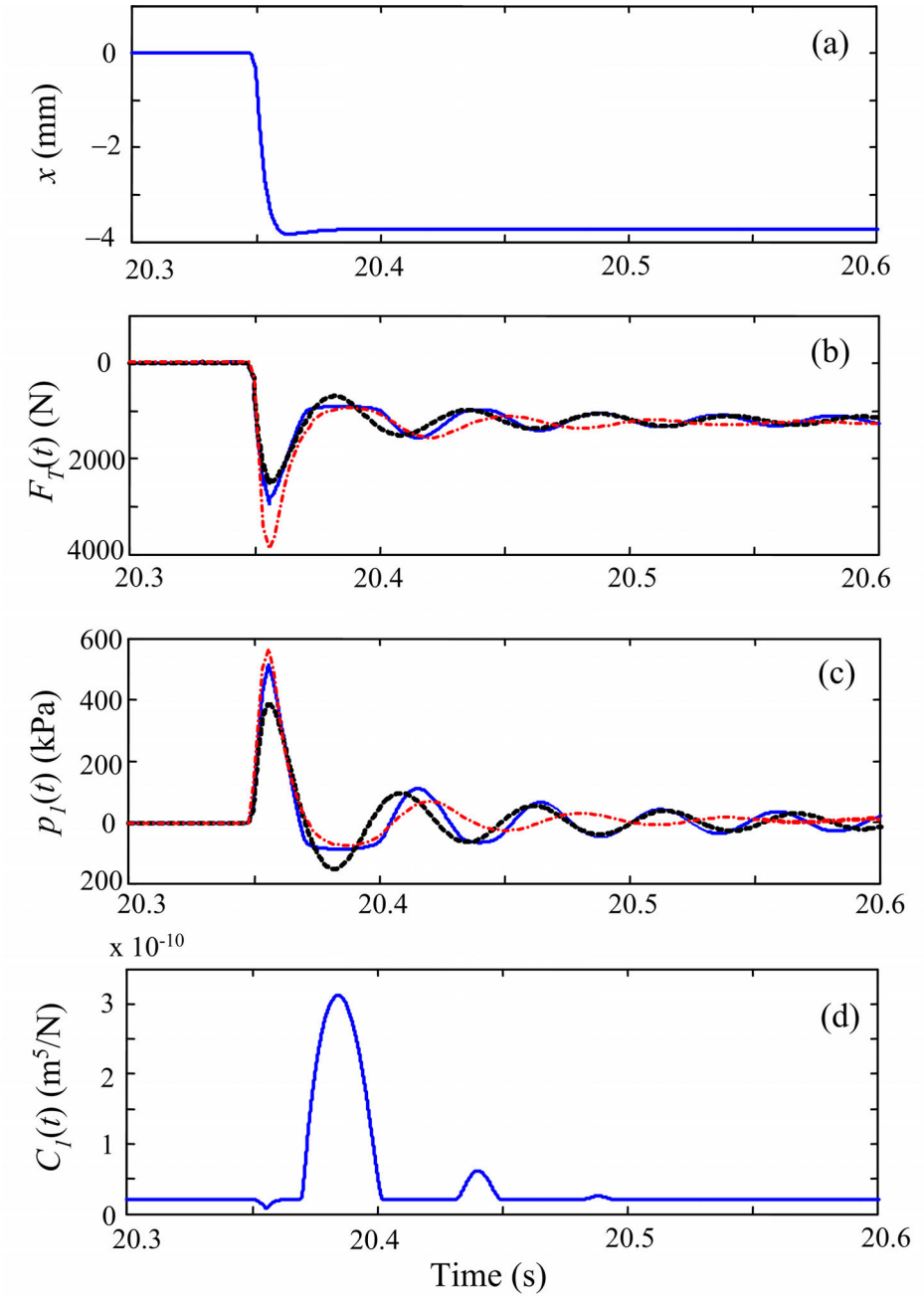


Fig. 4 Transient response of a fixed decoupler given step-down excitation mount: (a) displacement excitation $x(t)$ from 0 to -3.7 mm; (b) transmitted force $F_T(t)$ ; (c) top chamber pressure $p_1(t)$ ; and (d) multi-staged and time-varying $C_1(t)$ . Key for (b) and (c): ——, non-linear simulation using multi-staged $C_1(p_1)$ model; – – –, non-linear simulation using a constant $C_{10}$ ;– . –, measurement.

**6. Conclusion**

Chief contributions of this article include a historic review of the progress made in the identification of mount non-linearities, discussion of new discontinuous non-linearities ($C_1$ and $C_2$ models depending on the operating point(s) and/or dynamic loading) and prediction of the transient responses. Other contributions include a classification method for explicit displacement excitations (including a realistic profile) and implicit excitation that is introduced by the decoupler at the odd harmonics of the (explicit) fundamental frequency. New non-linear phenomena are explained in terms of the multi-staged (and time-varying) descriptions of $C_1$ and $C_2$. Finally, we successfully validate new or refined non-linear formulations by comparing predictions with measurements in terms of the top chamber pressure $p_1(t)$ and transmitted force $F_T(t)$. Results match well in both time and frequency domains. New formulations will be incorporated in vehicle dynamic models. Finally, this paper also shows that

considerable experimental and analytical work is often needed over a sustained period to diagnose and predict the non-linear behavior of real-life devices. Lessons learned in our work could be applied to other non-linear devices and systems.

**Acknowledgement**

We acknowledge the efforts of prior Acoustics and Dynamics Laboratory researchers whose work is still being analyzed and utilized: G. Kim, M. Tiwari, H. Adiguna and J. Sorenson.

**References**

[1] Singh R., Kim G. and Ravindra P. V., Linear analysis of an automotive hydro-mechanical mount with emphasis on decoupler characteristics, *Journal of Sound and Vibration*, 158(2), 219 - 243, 1992.

[2] Kim G. and Singh R., Non-linear analysis of automotive hydraulic engine mount, *American Society of Mechanical Engineers, Journal of Dynamic Systems, Measurement and Control*, 115, 482-487, 1993.

[3] Kim G. and Singh R., Study of passive and adaptive hydraulic engine mount systems with emphasis on non-linear characteristics, *Journal of Sound and Vibration*, 179(3), 427-453, 1995.

[4] Colgate J. E., Chang C. T., Chiou Y. C., Liu W. K. and Keer L. M., Modeling of a hydraulic engine mount focusing on response to sinusoidal and composite excitations, *Journal of Sound and Vibration*, 184(3), 503-528, 1995.

[5] Royston T. J. and Singh R., Vibratory power flow through a non-linear path into a multi-resonant receiver, *Journal of Acoustical Society of America*, 101(4), 2059-2069, 1997.

[6] Royston T. J. and Singh R., Study of Non-linear hydraulic engine mounts focusing on decoupler modeling and design, *SAE Transactions – Journal of Passenger Cars*, 106(2), 2759-2769, 1997.

[7] Jeong T. and Singh R., Inclusion of measured frequency-and amplitude-dependent mount properties in vehicle or machinery models, *Journal of Sound and Vibration*, 245(3), 385-415, 2001.

[8] Geisberger A., Khajepour A. and Golnaraghi F., Non-linear modeling and experimental verification of a MDOF hydraulic engine mount, *Control of Vibration and Noise-New Millennium*, 2000 ASME International Congress and Exposition, Nov. 5-10, 2000, Orlando, FL.

[9] Yu Y, Naganathan N. G. and Dukkipati R. V., A literature review of automotive vehicle engine mounting systems, *Journal of Dynamic Systems, Measurement, and Control*, 123(2), 186-194, 2001.

[10] Geisberger A., Khajepour A. and Golnaraghi F., Non-linear modeling of hydraulic mounts: theory and experiment, *Journal of Sound and Vibration*, 249(2), 371-397, 2002.

[11] Jazar G. N. and Golnaraghi M. F., Non-Linear modeling, experimental verification, and theoretical analysis of a hydraulic engine mount, *Journal of Vibration and Control*, 8(1), 87-116, 2002.

[12] Choi S. B. and Song H. J., Vibration control of a passenger vehicle utilizing a semi-active ER engine mount, *Journal of Vehicle System Dynamics*, 37(3), 193-216, 2002.

[13] Foumani M. S., Khajepour A. and Durali M., Application of sensitivity analysis to the development of high performance adaptive hydraulic engine mounts, *Journal of Vehicle System Dynamics*, 39(4), 257-278, 2003.

[14] Tiwari M., Adiguna H., and Singh R., Experimental characterization of a non-linear hydraulic engine mount, *Noise Control Engineering Journal*, 51(1), 36-49, 2003.

[15] Adiguna H., Tiwari M. and Singh R., Transient response of a hydraulic engine mount, *Journal of Sound and Vibration*, 268(20), 217-248, 2003.

[16] Foumani M. S., Khajepour A. and Durali M., A new high-performance adaptive engine mount, *Journal of Vibration and Control*, 10(1), 39-54, 2004

[17] He S. and Singh R., Estimation of amplitude and frequency dependent parameters of hydraulic engine mount given limited dynamic stiffness measurements, *Noise Control Engineering Journal*, 53(6), 271-285, 2005.

[18] Lee J. H. and Kim K. J., An efficient technique for design of hydraulic engine mount via design variable-embedded damping modeling, *Journal of Vibration and Acoustics*, 127(1), 93-99, 2005.

[19] He S and Singh R., Approximate step response of a non-linear hydraulic mount using a simplified linear model, *Journal of Sound and Vibration,* 2007 (in press).

[20] He S and Singh R., Discontinuous non-linearities in the hydraulic engine mount, submitted to *Journal of the Sound and Vibration*.